Turk J Agric For
29 (2005) 19-28

Using Advanced Spectral Analyses Techniques as Possible Means of Identifying Clay Minerals

Ünal ALTINBAŞ*, Yusuf KURUCU, Mustafa BOLCA
Ege University, Faculty of Agriculture, Soil Department, İzmir - TURKEY
A. H. El-NAHRY
National Authority for Remote Sensing and Space Sciences, Cairo - EGYPT

Received: 15.01.2004

Abstract: Spectral analyses, one of the most advanced remote sensing techniques, were used as a possible means of identifying the mineralogy of the clay fractions that corresponded to the Küçük Menderes Plain, south of İzmir, Turkey. Different spectral processes were used to execute the prospective spectral analyses. The processes include: i. the reflectance calibration of TM images belonging to the studied area, ii. using minimum noise fraction (MNF) transformation and iii. creating the pixel purity index (PPI), which was used to the most "spectrally pure", extreme, pixel in multi-spectral images. Spectral analyses of the clay mineralogy of the studied area were obtained by matching the unknown spectra of the purest pixels to pre-defined (library) spectra providing scores with respect to the library spectra. Three methods, namely Spectral Feature Fitting (SFF), Spectral Angle Mapper (SAM) and Binary Encoding (BE) were used to produce a score between 0 and 1, where the value of 1 equals a perfect match showing the exact mineral type. We were able to identify 4 clay minerals i.e., vermiculite, kaolinite, montmorillonite and illite, recording different scores related to their abundance in the soils. In order to check the validity and accuracy of the results obtained regarding the spectral signatures of the minerals identified, soil samples taken from the same localities were subjected to X- ray analysis. As a result a good correlation was found between the spectral signatures and the X- ray diffractions.

Key Words: Remote sensing, spectral analysis, X-ray diffraction, clay mineralogy.

İleri Spektral Analiz Teknikleri Kullanılarak Kil Minerallerinin Belirlenebilirliği

Özet: İzmir ilinin güneyinde bulunan Küçük Menderes deltası topraklarında kil mineral tiplerinin belirlenmesinde uzaktan algılama tekniklerinden spektral analiz tekniği kullanılmıştır. Bu amaçla çalışma alanına ait TM görüntülerinin yansıma kalibrasyonu yapılmıştır. Minimum Noise Fraction (MNF) yöntemi ile görüntüdeki bozukluklar gerekli matematiksel algoritmalar kullanılarak azaltılmıştır. Pixel Purity Index (PPI) tekniği kullanılarak görüntünün piksel boyutundaki mineral tanecik yansımaları belirlenmiştir. MNF ve PPI teknikleri beraberce kullanılmış ve 3 boyutlu görünüm yardımıyla en iyi yansımayı veren piksellerin yerini bulmak, tanımlamak ve sınıflandırarak ayrımlı mineraller için en iyi spektral yansımalar belirlenmiştir. Çalışma alanına ait bilinmeyen spektral yansıma analizleri minerallerin yansıma özellikleri ile karşılaştırılmıştır. Spectral Feature Fitting (SFF), Spectral Angle Mapper (SAM) ve Binary Encoding (BE) teknikleri kullanılarak spektral yansımalarla mineral yansımaları arasında eşleştirilme yapılarak ayrımlı mineral tipleri belirlenmiştir. Bu yöntemlerde 0 ile 1 arasında değişen sayılar kullanılmıştır. 1 en uygun eşlemeye karşılık gelen spektral özellik olup, bir mineralin spektral özelliğine tam olarak uyan yansımayı göstermektedir. Çalışma alanı topraklarında bulunma yoğunluğuna gore kil mineralleri vermikulit, kaolinit, illit ve montmorillonit'tir. Kullanılan spektral yöntemlerde bulunan minerallere ait spektral değerlerin doğruluk analizleri için spektral analizlerin yapıldığı alanlardan toprak örnekleri alınmış ve toprak örneklerinin X-ray sonuçları ile spektral analiz sonuçları arasında pozitif ilişki belirlenmiştir.

Anahtar Sözcükler: Uzaktan algılama, spektral analiz, X-ray difraktometresi, kil mineralojisi.

Introduction

The current work focused on a small portion of the Küçük Menderes valley for the identification of the mineralogy of clay samples. The study was in line with the philosophy of remote sensing, which is based on identifying objects or natural resources without physical connection remotely by the use of different sensors. The main objective of the current work was a trial to

* Correspondence to: altinbas@ziraat.ege.edu.tr

recognize the dominant clay minerals of the Küçük Menderes soils, by applying the highly advanced remote sensing techniques of spectral analyses.

Olsen et al. (2000) described research aimed at determining the feasibility of using reflectance spectroscopy to identify and characterize the expansive clays and clay-shales along the Colorado Front Range Urban Corridor, both at the laboratory/field scale, and at the remote-sensing scale.

Chabrillat et al. (2001) established the correlation of clay mineralogy with swelling potential indices and the expansion of existing correlations of laboratory reflectance spectra with clay mineralogy, examining also direct correlations between reflectance data and swelling potential.

Materials

The Küçük Menderes valley occupies about 400 km^2 in the western part of Turkey. It is located between 37º 45´ and 38º 00´ N latitudes and between 27º 15´ and 28º 30´ E longitudes. The valley represents the most important agricultural area, the south part of the city İzmir. The valley is surrounded by highlands acting together as catchments areas that supply the Küçük Menderes river tributaries with rainwater and weathered materials. The valley is separated from the other neighboring valleys by 2 mountainous chains, which define its natural boundaries. Near the Aegean coast the Küçük Menderes penetrates a narrow valley, forming a delta near the city of Selçuk, where the meanders drain into the Aegean Sea.

Methods

Digital image processing

Image processing using ENVI 3.4 software includes the following processes:

a) Calibration of a Landsat 7 (taken in 2003) ETM image to reflectance. Filtering by the adaptive filters to reduce noise by smoothing while preserving sharp edges. b) Stretching using Gaussian stretching methods using a mean DN of 127 with the data values of 3 standard deviations set to 0 and 255. c) Geometric correction using image to image methods for adding ground control points with 3 m average RMSE and nearest method use as a resampling method, and image projection using the Universal Transverse Mercator (UTM).

Fieldwork

A reconnaissance survey was conducted in the investigated area in order to gain an appreciation of the broad soil patterns according to the obtained spectra end members. GPS Garmin12XL (+-,5-8 m) was used in the field to recognize the accurate locations of the end members for soil sampling. Four surface soil samples representing the major soils in the area were collected for X-ray diffraction analyses.

Using USGS Spectral Library (Minerals)

The spectra that represent the USGS spectral library were measured on a custom-modified, computer-controlled Beckman spectrometer at the USGS Denver Spectroscopy Lab., U S A. Wavelength accuracy was in the order of 0.0005 µm (0.5 nm) in the near-IR and 0.0002 µm (0.2 nm) in visible light (http://speclab.cr.usgs.gov/spectral-lib.html).

X-Ray Diffraction Analyses

The clay fraction was separated after being pretreated according to the procedure described by Jackson (1975). The clay samples were X-rayed after they had been Ca-saturated at 25 °C, Ca-saturated and glycolated, and K-saturated at 25 °C. Apart from the above treatment, sample no. 1 (Ca-saturated) was also heated to 300 °C and 520 °C.

X-ray diffraction patterns were obtained with the Philips P.W. (1060/100) X- ray diffractometer with Cu-α radiation and an iron filter. Identification of the clay minerals was carried out following the guidelines provided by Black (1965), MacEwan (1980), Carroll (1970) and Weed (1977).

Results and Discussion

Many obstacles and atmospheric and environmental conditions (i.e., weathering processes) are still hampering the accurate identification of land resources due to their influence on the accuracy of measured spectra. Thus, the tool of spectral analyses is not foolproof. Nevertheless, it is meant to be used as a starting point for identifying materials in an image scene. When used properly, spectral analysis tools in conjunction with a good spectral library could provide excellent suggestions for identification of objects on the land surface. Spectral analyses were used to identify the clay minerals of the Küçük Menderes soils using the following procedures.

Display of Color Composite ETM Image

1. A color composite ETM image has been filtered to produce output images in which the brightness value at a given pixel is a function of some weighted average of the brightness of the surrounding pixels.

2. Enhanced and stretched. The results obtained from Gaussian stretching improved the visual display of the spectra information as shown in Figure 1

3. Geometrically corrected and displayed using a band combination of 3 2 1 (RGB - true color) as shown in Figure 2.

Calibration of the ETM Image

A reflectance calibration was required for Landsat ETM data to compare image spectra with library reflectance spectra and to run some Minimum Noise Fraction (MNF) and Pixel Purity Index (PPI) routines. ETM image calibration was been used with pre-launch gains and offsets calculated for Landsat sensors (Markham and Barker, 1986).

Minimum Noise Fraction

MNF transformation is a method similar to principal components. It was used to determine the inherent dimension of the image data, to segregate noise in the data, and to reduce the computational requirements for subsequent processing (Boardman and Kruse, 1994). The MNF is used as a preparatory transformation to put most of the essential components into just a few spectral bands and to order those bands from the most interesting (that can segregate noise perfectly) to the least interesting. Two cascaded principal components transformations were implemented in the current work. The first

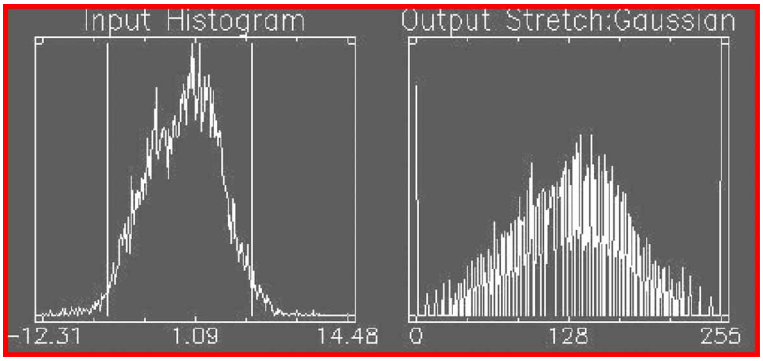

Figure 1. Gaussian-stretching results of TM image.

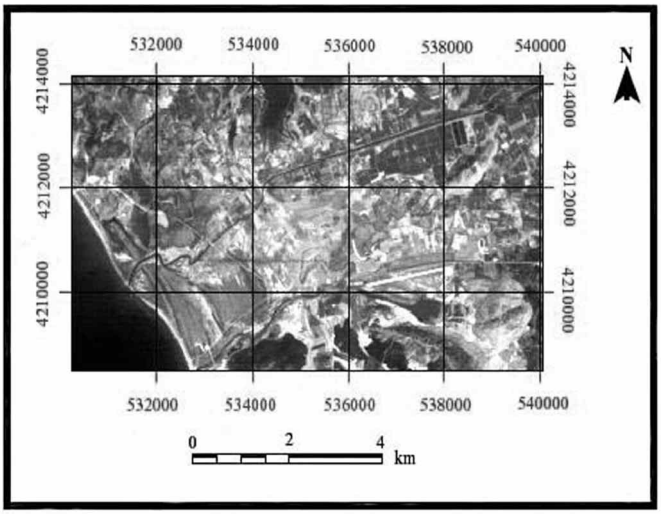

Figure 2. The true color composite 3 2 1 of the investigated area.

transformation, based on an estimated noise covariance matrix, decorrelates and rescales the noise in the data. This first step results in transformed data in which the noise has unit variance and no band-to-band correlations. The second step is a standard principal components transformation of the noise-whitened data. For the purposes of further spectral processing, the inherent dimension of the data is determined by the examination of the final eigenvalues (of noise segregation) and the associated image bands. The data space could be divided into 2 parts: one part associated with large eigenvalues and coherent eigenimages, and a complementary part with near unity eigenvalues and noise dominated images. By using only the coherent portions, the noise was separated from the data, thus improving spectral processing results. The decreasing eigenvalue with increasing MNF band as shown in the eigenvalue plot in Figure 3 shows how noise is segregated in the higher number MNF bands and it was noted that there was a decrease in spatial coherency with increasing MNF band number as shown in Figures 4 and 5.

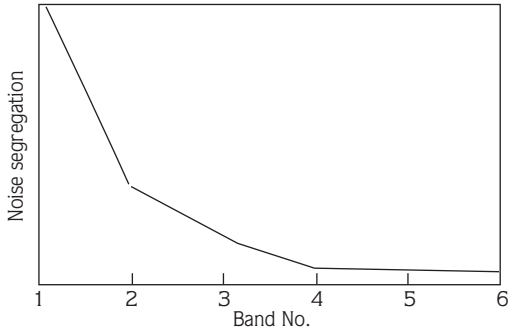

Figure 3. Noise segregation plot.

Figure 4. MNF band 1.

Figure 5. MNF band 6.

Pixel Purity Index

The PPI function finds the most spectrally pure or "extreme" pixels in multispectral and hyperspectral data (Boardman and Kruse, 1994; Boardman et al., 1995). The extreme pixels correspond to the materials with spectra that combine linearly to produce all of the spectra in the image. The PPI was computed by using projections of n-dimensional scatter plots to 2-D space and marking the extreme pixels in each projection. The extreme pixels in each projection were recorded and the total number of times each pixel was marked as extreme was noted. The output is an image (the PPI image) in which the digital number (DN) of each pixel in the image corresponds to the number of times that pixel was recorded as extreme. Thus, bright pixels in the image showed the spatial location of spectral endmembers. Image thresholding was used to select several thousand pixels for further analysis, thus significantly reducing the number of pixels to be examined (Figure 6).

The PPI, as shown in Figure 7, indicated the total extreme pixels for the studied area, whereas 5212 pixels were recorded throughout iteration no. equal to 4000 times for a pixels threshold of 3.

Chabrillat et al. (2002) used AVIRIS and HyMap images acquired recently with a high signal-to-noise ratio (SNR) to detect clays. The results showed the extent to which laboratory spectra of swelling soils field samples could be used to detect and discriminate different clays, smectite, illite and kaolinite, related to variable swelling potential.

Goetz et al. (2001) and Olsen et al. 2000 used near-infrared reflectance spectroscopy to discriminate among

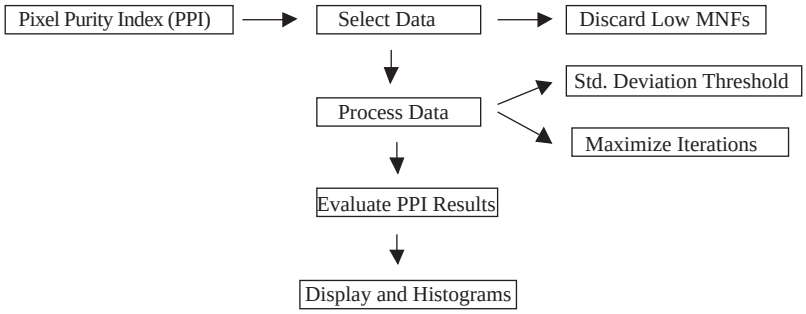

Figure 6. Flow chart of the PPI procedures.

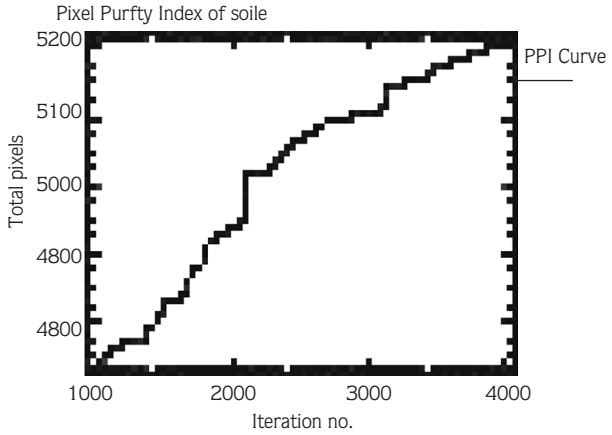

Figure 7. PPI index.

Figure 8. PPI map.

pure smectite and mixed-layer I/S samples, based on characteristic absorption bands in the 1900–2400 nm spectral region.

The following single band images, as seen in Figures 8 and 9, represent the PPI, where the extreme (purest) pixels are white in Figure 8. It is noted that the extreme pixels occupied the region of interest, as shown in Figure 9.

n-Dimensional Visualization and Extracted Endmember Spectra

The n-D visualization was used in conjunction with the MNF and PPI tools to locate, identify and cluster the purest pixels and the most extreme spectral responses in a data set. If spectral signatures are recorded properly and the curve shape is accurate they could be used for remote sensing applications (Salisbury et al., 1991).

Spectra can be thought of as points in a dimensional scatter plot, where n is the number of bands (Boardman

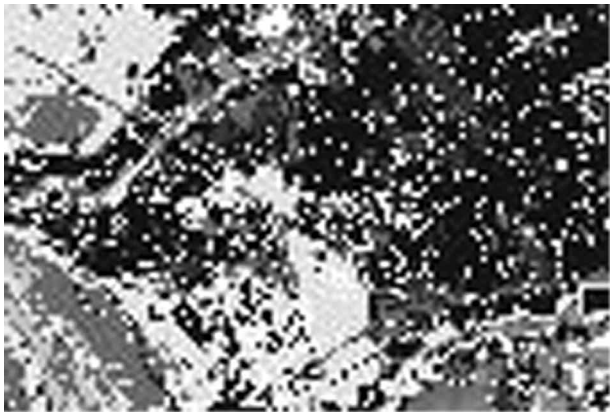

Figure 9. Region of interest.

et al.,1995). The coordinates of the points in n-space consists of "n" values that are simply the spectral radiance or reflectance values in each band for a given pixel. The distributions of these points in n-space were used to estimate the number of spectral endmembers (4

highlighted segmentations), as shown in Figure 10, producing 4 pure spectral signatures, which were extracted and plotted in an n-D visualizer plot representing the selected endmembers, as shown in Figure 11.

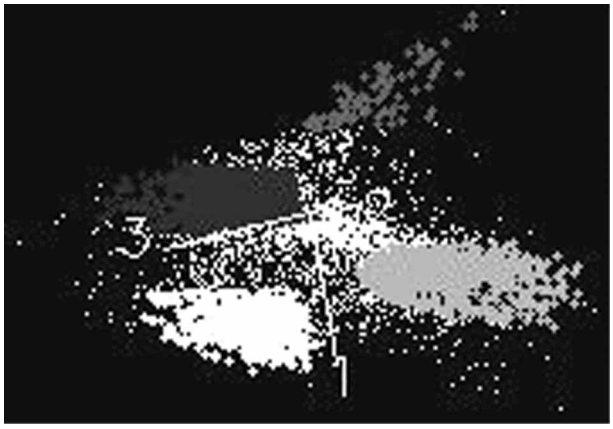

Figure 10. 3-D visualization.

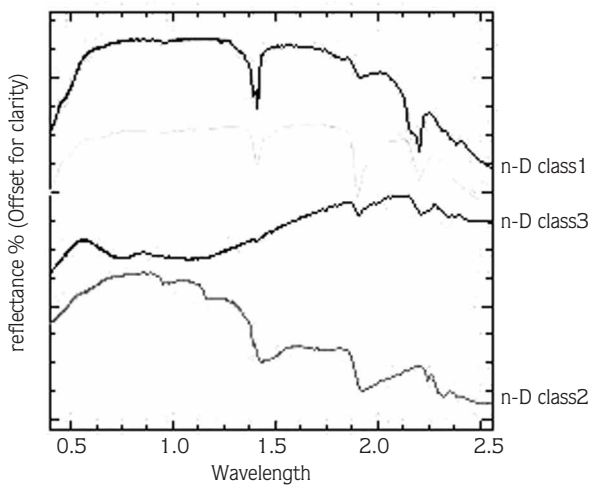

Figure 11. Classes of the selected spectra.

Matching Unknown Spectra to Library Spectra

Spectral analyses and consequently clay mineral identification could be obtained by matching the unknown spectra extracted from the 3-D visualizer to pre-defined (library) spectra, providing scores with respect to the library spectra. Three weighting methods, i.e. Spectral Feature Fitting (SFF), Spectral Angle Mapper (SAM) and/or Binary Encoding (BE), were used to identify mineral type, producing a score between 0 and 1, where 1 equals a perfect match. As is known, some minerals are similar in one wavelength range, yet very different in another. For the best results, a wavelength range that contains the diagnostic absorption features was used to distinguish among the minerals.

De Jong's (1992) correspondence analysis of the spectral characteristics of soils revealed lime, clay, iron and organic matter as the important variables, and pH and the absorption features of Illite are generally broader and less well defined compared with those of muscovite. Nevertheless, the illite, muscovite and montmorillonite spectra have similar absorption bands. Illite {(K,H,O)(Al,Mg,Fe), (Si,Al),O,,((OH),,H,O)} shows broad water absorption features near 1.4 and 1.9 ym, and additional Al-hydroxyl features at 2.2, 2.3 and 2.4 pm. Illite and muscovite have absorption bands near 2.35 and 2.45 pm, that are lacking in the montmorillonite spectrum.

The output of the spectral analysis is a ranked score or weighted score for each of the materials in the input spectral library, as shown in Table 1. The highest score indicates the closest match and shows higher confidence in the spectral similarity, where illite/smectite and kaolinite, scored high values of 1.0 and 0.944,

Table 1. Weighting methods and mineral type/score of the extracted spectra.

Spectra class	Weighting Method (Score 0-1.0)					
	SAM		SFF		BE	
	Mineral type	Score	Mineral type	Score	Mineral type	Score
1	-	0	Kaolinite	0.944	Kaolinite	0.833
2	-	0	Vermiculite	0.833	Vermiculite	0.667
3	-	0	Illite/Smectite	1.000	Illite/Smectite	0.883
4	-	0	Montmorillonite	0.667	Montmorillonite	0.500

respectively, while vermiculite and montmorillonite scored 0.833 and 0.667, respectively, using SFF weighting. The same clay minerals recorded scores of 0.833, 0.833, 0.667 and 0.500, respectively, using BE weighting. On the other hand, the SAM did not recognize any kind of clay minerals (zero score).

According to Altınbaş (1982), using X-ray analysis, illite and kaolinite were the dominant clay minerals in the acidic brown forest soils (Typic Dystrustrepts), followed by vermiculite and montmorillonite. Basically, the clay minerals found in these soil groups are products of the transformation and decomposition of biotite, muscovite and feldspars. In order to check the validity and accuracy of our results concerning spectral signatures and to define perfectly, the existing clay minerals, X-ray diffraction analysis was the obvious choice. The results obtained from X-ray diffraction indicated that the clay fraction contained mainly illite and kaolinite as the dominant clay minerals, followed by vermiculite and montmorillonite and small amounts of other minerals (Figures 12-16).

Mermut et al. (1997) found that the soil loss from a soil dominated by smectite was high. The splash and wash erosion in 80 mm of rain were 23 and 2.1 Mg ha-1, respectively, in a loamy soil in which smectite, mica and vermiculite were the dominant clays, and 7.3 and 0.91 Mg ha-1 respectively, in a silt loam soil in which vermiculite, mica and kaolinite were dominant.

Illite

Illite as a 2:1 clay mineral was recorded in the X-ray diffractogram at 10.04 Å. Illite is a widespread mineral in Kücük Menderes soils (Altınbaş, 1982). It may be formed by the alteration of mica minerals. Illite was found as the dominant clay mineral by X-ray analysis in the acidic brown forest soils, which were developed on mica schist

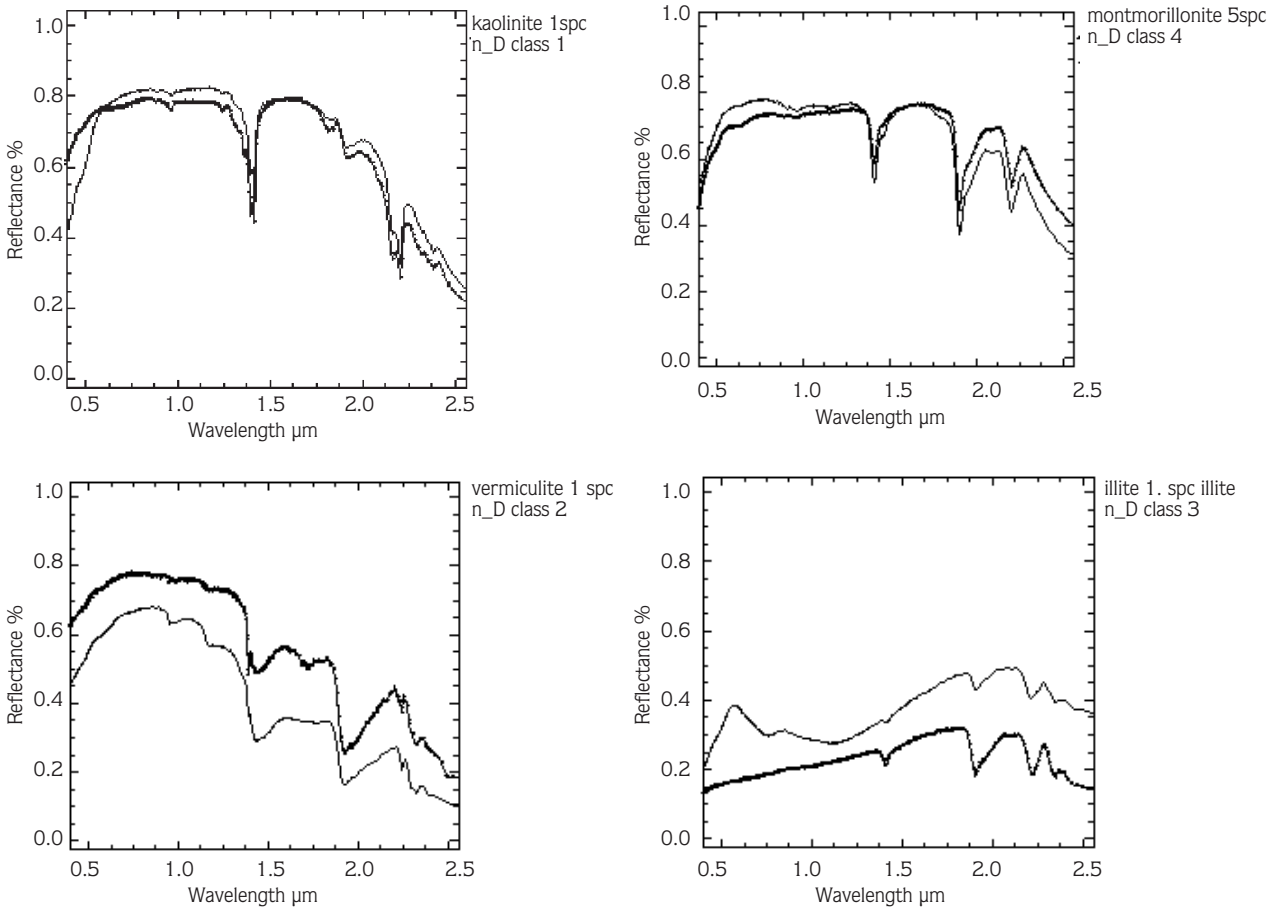

Figure 12. ID of kaolinite, illite, montmorillonite and vermiculite.

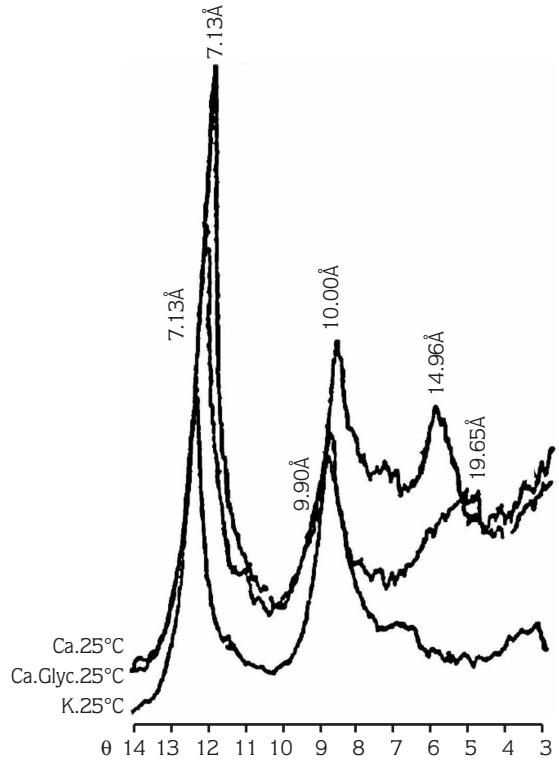

Figure 13. X-ray diffraction of the clay fractions-sample no.1 (0-4 cm) with Ca^{++}, K^{+}, Ca^{++}+Glyc. at 25 °C.

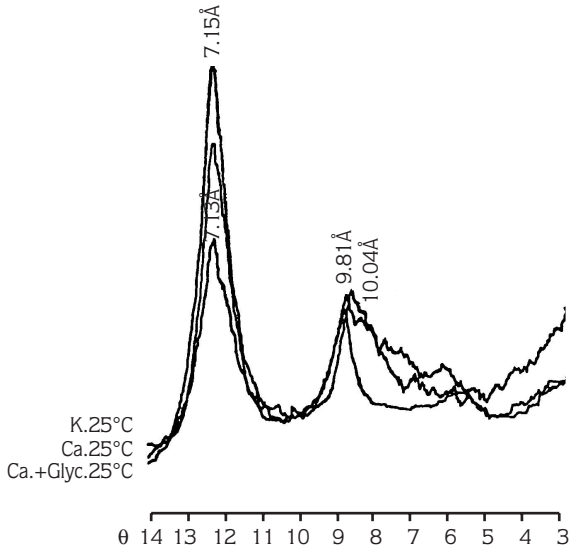

Figure 14. X-ray diffraction of the clay fractions-sample no. 2 (0-6 cm) with Ca^{++}, K^{+}, Ca^{++}+Glyc at 25 °C.

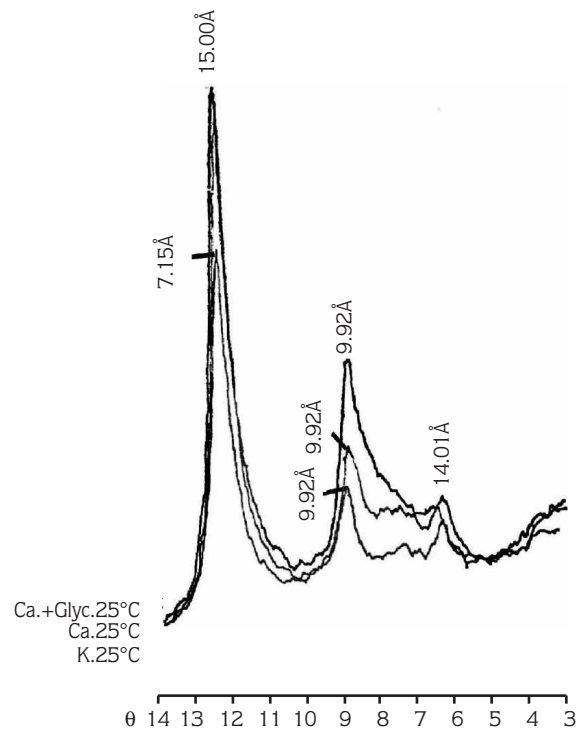

Figure 15. X-ray diffraction of the clay fractions-sample no. 3 (0-5 cm) with Ca^{++}, K^{+}, Ca^{++}+Glyc at 25 °C.

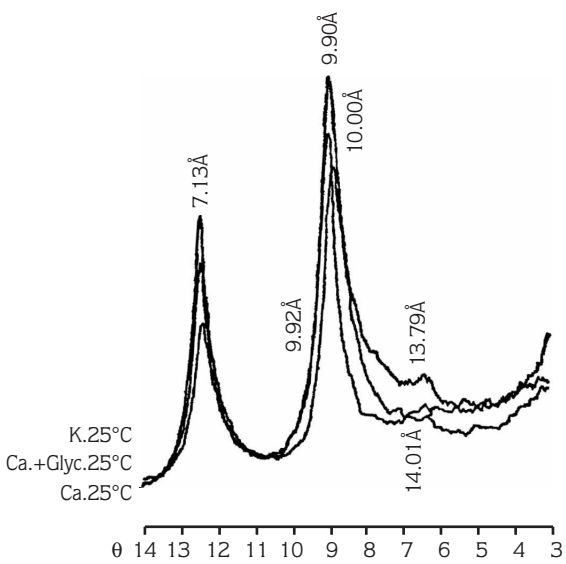

Figure 16. X-ray diffraction of the clay fractions-sample no. 4 (0-7 cm) with Ca^{++}, K^{+}, Ca^{++}+Glyc at 25 °C.

parent material similar to that of Kücük Menderes (Altınbaş, 1982).

Kaolinite

Kaolinite is a 1:1 clay mineral, the presence of which was shown by the strong peak at 7.13 Å (25 °C with K-saturation). The peak disappeared only after heating to 520 °C. The presence of kaolinite confirms the hydromorphic condition of the soils and its inheritance from parent materials. Kaolinite may be formed by the weathering of K-feldspars and Na-feldspars from magmatic and metamorphic rocks or by a hydrothermal attack of acid solutions on feldspars and micas. Kaolinite is common in Kücük Menderes soils. Kaolinite also may be formed by the silicification of hydrargillite by silicic acid solutions (Altınbaş, 1982).

Vermiculite

Vermiculite, a 2:1 clay enriched with Mg, was identified by the presence of the 14.96 Å peak (Ca-saturated and glycolated), which shifted to 10.04 Å after Ca- saturation and heating to 520 °C. The presence of this mineral is explained on the premise that Mg-affected conditions stimulate its formation either through digenesis or through neogenesis. This mineral is not as widespread as illite in these soils. It may be formed by hydrothermal action on biotite in a magnesium–rich environment. After erosion, the mineral is found in the clay fraction of fluvial sediments. Vermiculite was found in smaller amounts compared with illite and kaolinite in the acidic brown forest soils that developed on mica schist on the highlands that surround the study area (Altınbaş, 1982).

Montmorillonite

Montmorillonite is a 2:1 clay mineral formed as a result of the hydrothermal alteration of volcanic ashes. The extreme thinness and flexibility of the flake-shaped particles account for the plasticity of this mineral (Altınbaş, 1982).

Montmorillonite reflected at 19.65 Å. [The mineral of this group consists of unit layers formed by 1 Al (Mg, Fe, Zn, Cr, Li) – OH octahedral sheet and with 2 Si(Al, Fe)-O tetrahedral sheets]. The pattern indicates basal reflection at about 14.96 Å for Ca-saturated samples, which expanded to 17.65 Å upon glycerol salvation with a second basal reflection. The peak collapsed to 9.92 Å upon Ca-saturation and heating for 4 h at 520 °C. This mineral reflects the contribution of water to soil formation and its formation is favored by alkalies and alkaline earth's enrichment of the pedo-environments. Montmorillonite is inherited from parent materials prior to sedimentation (Altınbaş, 1982).

Conclusions

1. The MNF method put most of the information into a few spectral bands to reduce the volume of data and to segregate the noise.

2. The PPI is a means of finding the most "spectrally pure" pixel. The output is an image in which the DN of each pixel in the image corresponds to the number of times that pixel was recorded with iteration running as extreme, thus significantly reducing the number of pixels.

Both the MNF and PPI operations effectively reduce the data volume to be analyzed interactively. The PPI image is used as an input for n-dimensional scatter plotting that allows real time rotation in n-dimensions. The n-D visualizer for image clustering was performed to create classes (endmembers) by clustering the purest pixels in the data set. Animation of the scatter-plots of bands was used to select the endmembers. The results show that there are 4 classes can be distinguished by grouping pixels. After the classes were defined by clustering, the selected classes were exported as regions of interest and matched with the spectral library, resulting in 4 classes representing different types of clay minerals of kaolinite, montmorillonite, vermiculite and illite.

3. N-Dimensional visualization for image clustering using scatter plotting animation was performed.

4. Using the spectra extracted from the ETM image with the aid of hyperspectral tools (MNF, PPI and N-dimensional visualization) clay mineral type on the soil surface can be identified.

Recommendations

The success of this effort implies that spectral signatures can be used broadly and economically for identifying clay minerals. Such an effort should concentrate on automating image analysis to permit the analysis of large volumes of data in a short time. When implemented, the spectral signatures approach can be used to supplement (and in some cases possibly even replace) the X-ray analysis of clay minerals and potentially bring new information to the spectra used in a variety of soil subdisciplines.

References

Altınbaş Ü. 1982. Potassium minerals in acidic brown forest soils developed on micaschist in Bozdağ (Brown Mountains) and their sources and their effects on the soil potassium reserves. Ege Univ. Faculty of Agriculture Press. No. 433. İzmir, Turkey.

Black, C.A. 1965. Methods of soil analyses Part 1. Physical and mineralogical properties American Society Agronomy, Inc. Pub. Madison,Wisconsin U.S.A.

Boardman J. W. and F. A. Kruse, 1994. Automated spectral analysis: A geologic example using AVIRIS data, north Grapevine Mountains, Nevada: in Proceedings, Tenth Thematic Conference on Geologic Remote Sensing, Environmental Research Institute of Michigan, Ann Arbor, MI, p.I-407-I-418.

Boardman J.W., F.A. Kruse and R.O. Green, 1995. Mapping target signatures via partial unmixing of AVIRIS data: in summaries, Fifth JPL Airborne Earth Science Workshop, JPL Publication 95-1, v.1p.23-26.

Carroll, D., 1970. Clay minerals. A guide to their X-ray identification. Geological Society of America. Spec. page 126, Boulder, Colorado, U.S.A.

Chabrillat, S., A.F.H Goetz, H.W. Olsen,, L. Krosley and D.C. Noe, (2002). Near-infrared spectra of expansive clay soils and their relationships with mineralogy and swelling potential. Clays and Clay Minerals (in revision).

De Jong, S.M. 1992. The analysis of spectroscopical data to map soil types and soil crusts of Mediterranean eroded soils. Soil Technology 5: p 199-211.

Goetz, A.F.H., S. Chabrillat and Z. Lu, (2001). Field reflectance spectrometry for detection of swelling clays at construction sites. Field Analytical Chemistry and Technology, 5: 143–155.

Jackson, M.L. 1975. Soil chemical analyses advanced course, Pub. by author, Madison, Wisconsin.

MacEwan, D.M.C. and Wilson, M.J. (1980) Interlayer and intercalation complexes of clay minerals. In G.W. Brindley and G. Brown, Eds.., Crystal Structures of Clay Minerals and their X-ray Identification, chapter 3, Monograph 5 of Mineralogical Society, London.

Markham, B.L. and J.L. Barker, 1986, Landsat MSS and TM Post-Calibration Dynamic Ranges, Exoatmospheric Reflectances and At-Satellite Temperatures, EOSAT Landsat Technical Notes, August 1986, p. 3-8, U S A.

Mermut, A.R., S.H. Luk, M.J.M. Romkens and J.W.A. Poesen, 1997. Soil loss by splash and wash during rainfall from two loess soils. Geoderma 75: 203–214.

Olsen, H.W., L. Krosley, K. Nelson, S. Chabrillat, , A.F.H. Goetz and Noe, D.C. (2000). Mineralogy-swelling potential relationships for expansive shales. In C.D. Shackelford, S.L. Houston and N.-Y. Chang (Eds.), Advances in unsaturated geotechnics (Geotechnical Special Publication 99, pp. 361– 378). Reston, VA: ASCE.

Salisbury, J.W., L.S. Walter, N. Vergo and D.M. D'Aria, 1991. Infrared (2.1-25 micrometers) Spectra of Minerals" Johns Hopkins University Press, Baltimore.

Weed, S.B., 1977. Minerals in soil environment. Soil Science Society of America Journal, 56: September-October 1977: 1640-1645.